Clay-coated sand grains in petroleum reservoirs: understanding their distribution via a modern analogue

L. J. Wooldridge*[1], R. H. Worden*[2], J. Griffiths, J. E. P. Utley

[1]*School of Environmental Sciences, University of Liverpool, Liverpool L69 3GP, UK*

*[1]*Corresponding authors (e-mail:* luke.wooldridge@liv.ac.uk*)*

*[2]*Corresponding authors (e-mail:* r.worden@liv.ac.uk*)*

ABSTRACT

Clay coated grains can inhibit ubiquitous, porosity-occluding quartz cement in deeply buried sandstones and thus lead to anomalously high porosity. A moderate amount of clay that is distributed in sandstones as grain coats is good for reservoir quality in deeply buried sandstones. Being able to predict the distribution of clay coated sand grains within petroleum reservoirs is thus important to help find and exploit such anomalously good reservoir quality. Here we have adopted a high resolution, analogue approach, using the Ravenglass Estuary marginal-shallow marine system, in NW England, UK. Extensive geomorphic mapping, grain size analysis and bioturbation intensity counts were linked to a range of scanning electron microscopy techniques to characterise the distribution and origin of clay-coated sand grains within surface sediment. Our work shows that grain coats are common within this marginal-shallow marine system but they are heterogeneously distributed as a function of grain size, clay fraction and depositional facies. The distribution and characteristics of detrital-clay coated grains can be predicted with knowledge of specific depositional environment, clay fraction percentage and grain size. The most extensive detrital-clay coated grains are found within sediment composed of fine-grained sand containing 3.5 to 13.0 % clay fraction, associated with inner estuary tidal flat facies. Thus, against common convention, the work presented here suggests that, in deeply buried prospects, the best porosity may be found in fine-grained, clay-bearing inner tidal flat facies sands and not in coarse, clean channel fill and bar facies.

INTRODUCTION

Porosity and permeability generally decrease with increasing depth of burial in sandstones, although a significant number of deeply buried sandstone reservoirs have unusually high porosity and permeability (Bloch et al. 2002). Such anomalously high porosity and permeability have most commonly been linked to the presence of chlorite clay coated grains that inhibit the growth of porosity-occluding quartz cement (Ajdukiewicz and Larese 2012; Ehrenberg 1993; Worden and Morad 2000).

The term clay coat encompasses both detrital and diagenetic origins (Ajdukiewicz and Larese 2012). Detrital-clay coated grains occur at or near the surface of the sediment, and are the primary focus of this study.

Diagenetic clay coats either develop from the thermally-driven recrystallization of low-temperature, detrital precursor clay coats or they grow in situ due to the authigenic alteration of detrital or early diagenetic minerals interacting with the pore fluids during burial (Ajdukiewicz and Larese, 2012; Wise et al., 2001; Worden and Morad, 2003).

Chlorite and illite clay coatings are considered to preserve reservoir quality by reducing the nucleation area on detrital quartz grains that is available for authigenic quartz cementation (Ehrenberg 1993; Pittman et al. 1992). Porosity can be at least 10 % higher than expected where grain-coating clays are abundant (Ehrenberg 1993). Experiments undertaken by Ajdukiewicz and Larese (2012); Billault et al. (2003) and Lander et al. (2008) led to the conclusion that clay crystals within the clay coat act as barriers, inhibiting epitaxial quartz cement growth and subsequent coalescence to form thick quartz overgrowths. The primary factors controlling the effectiveness of clay coated grains for the inhibition of authigenic, porosity-occluding quartz cement are the extent, completeness and distribution of the detrital precursor clay coated grains (Billault et al. 2003).

Oil field-based studies which collectively show that clay coats are most common in fluvial to marginal marine sediments including: Jurassic sandstones on the Norwegian continental shelf (Bloch et al. 2002), Jurassic-Triassic fluvial, lacustrine-deltaic sandstones of the Ordos basin, China (Luo et al. 2009), marginal marine Jauf Formation, eastern Saudi Arabia (Al-Ramadan et al. 2004), the Upper Cretaceous Tuscaloosa Formation, USA (Pittman et al. 1992), and see review by Dowey et al. (2012). However there is no model capable of predicting the occurrence of clay coated grains or the degree of completeness of grain coats within fluvial to marginal marine sediments.

The positive influence of chlorite and illite clay-coated grains on reservoir quality in deeply buried sandstone has resulted in extensive reservoir core-based research (Ajdukiewicz et al. 2010; Gould et al. 2010; Pittman et al. 1992) and laboratory experiments (Ajdukiewicz and Larese 2012; Billault et al. 2003; Pittman et al. 1992). Chlorite coated grains have been observed to inhibit quartz cement and the need to understand the origin of chlorite coated grains was the driving force that led to the current study. Notable chlorite clay coated reservoir units include the Tilje Formation, Norwegian continental shelf (Ehrenberg 1993), Tuscaloosa Formation, U.S. Gulf Coast (Ajdukiewicz and Larese 2012) and the Rotliegend Sandstone, northern Netherland (Gaupp and Okkerman 2011). Sandstones which contain illite and mixed layer illite-smectite clay coated grains have been less commonly advocated but include the Garn Formation, Mid-Norway (Storvoll et al. 2002), Williams Fork Formation, Colorado (Ozkan et al. 2011) and Jauf Formation, Eastern Saudi Arabia (Al-Ramadan et al. 2004; Cocker et al. 2003).

Aagaard et al. (2000) showed that low temperature, discontinuous, detrital-clay coated grains recrystallized during experiments at 90 °C to form thick, continuous, diagenetic clay coats that are morphologically consistent with naturally occurring reservoir examples. In some examples, euhedral clay minerals grow out into the pore from an underlying, unstructured clay coat (Gould et al. 2010). Such clay coat stratigraphy could be the result of a detrital, or very early diagenetic, clay coat acting as a seed for deep burial diagenetic clay coat neoformation.

Despite the importance of being able to predict the occurrence and distribution of detrital-clay coated grains, there is no all-encompassing model that is useful for ranking prospects or populating reservoir models with the completeness of clay coats in marginal marine sandstones. Relatively little fundamental work has been undertaken on the controls on clay coat growth in sediments although Wilson (1992) and Matlack et al. (1989) undertook early studies focused upon environments (aeolian, marine-shelf, marginal marine, fluvial) in which clay-coated sand grains occur and potential mechanisms of formation (bioturbation, infiltration, inheritance). In order to predict anomalously high porosity in the subsurface, there is a need to focus on the origin and spatial distribution of detrital-clay coated grains since clay coats inhibit quartz cement in deeply buried sandstones (Bloch et al. 2002) Anomalously high porosity has also been shown to derive from other possesses such as early oil charge, over pressure and microquartz coatings (Bloch et al. 2002).

The four main ways to develop a fundamental understanding of primary sedimentary environment and mineral distribution, and thus the processes that lead to clay coats, are: core-based studies, outcrop based studies, experimental studies and modern analogue studies. Core based studies have problems of limited spatial resolution of samples (wide spacing between wells and the lack of abundant cores in most fields) and the abiding uncertainty about both the primary mineralogy and exact environment of deposition due to subsequent diagenetic modifications. Outcrop based studies overcome the spatial resolution problem but typically suffer from weathering-related recent changes to mineralogy, plus outcrop-diagenesis studies routinely have problems in seeing through the long history of burial, heating and then uplift. We have here adopted a modern analogue approach, linking the distribution of detrital-clay coated grains to sedimentary processes and characteristics (grain size, percentage clay fraction) and biological processes (bioturbation). The detailed study of sediment from modern environments permits a high resolution investigation into the distribution of detrital-clay coated grains, removing the limited spatial distribution, stratigraphic coverage and ambiguous depositional environment interpretations of subsurface core-based studies. This study addresses the following questions, focussed on the marginal-shallow marine Ravenglass Estuary system (Fig. 1).

1. What are the textural characteristics of detrital-clay coated grains within a modern marginal-shallow marine setting?
2. What are the mineralogical characteristics of clay-coated sand grains within a modern marginal-shallow marine setting?
3. How variable is the coverage of detrital-clay coated grains within a modern marginal marine system?
4. What controls the formation and distribution of detrital-clay coated grains?
5. Are the clay coats in this modern, marginal-shallow marine system, texturally comparable to other modern or subsurface examples?
6. What is the potential impact of using modern analogues for the prediction of reservoir quality in ancient and deeply buried sandstones from the same primary environment?

STUDY SITE GEOMORPHOLOGY

The Ravenglass Estuary is located in Cumbria, NW England. The mid to upper portions of the Ravenglass Estuary are fed by three rivers the Esk, Mite and Irt, with the lower, western part of the estuary connected by a single channel to the Irish Sea (Bousher 1999) (Fig. 1). Ravenglass sediment is quartz-dominated (Daneshvar 2011; Daneshvar and Worden 2016) with depositional environments translatable to marginal-shallow marine petroleum reservoirs. Ravenglass is a modern analogue equivalent to the environment of deposition for many ancient and deeply buried, chlorite-coated sandstone reservoirs such as the tidally-influenced, shallow marine-deltaic Tilje Formation, Norway (Ehrenberg 1993), braid delta margin with foreshore and shoreface deposits Garn Formation, Norway (Storvoll et al. 2002), and shallow-marine to deltaic Lower Vicksburg Formation, USA (Grigsby 2001).

The 5.6 km^2 estuary has a maximum tidal range of 7.55 m and is 86% intertidal (Bousher 1999; Lloyd et al. 2013). The estuary has extensive back barrier tidal flats and tidal bars, fringed by well-established saltmarsh vegetation (Bousher 1999). The estuary is connected to the Irish Sea through a single, 500m wide, tidal inlet that dissects a fringing coastal barrier which is topped with eolian dunes. The three fluvial channels, fluvial overbank, foreshore and ebb delta complex provide a complete fluvial to marine transect that we have investigated in terms of depositional environments, and detrital-clay coat abundance, with analysis of detrital-clay coat mineralogy (Fig. 1). Despite the high spring tidal range, the estuary contains geomorphological elements consistent with a mixed energy (wave-tide) regime, following the estuary classification scheme proposed by Ainsworth et al. (2011). This indicates a tidal hydrodynamic dominance within the inner estuary and wave-dominated processes occurring along the foreshore coastal side of the barrier spits.

The marginal- shallow marine Ravenglass system can be divided into fluvial-, estuary-, shallow marine- and eolian dune-dominated regimes, with the results of this study subdivided by sub-environment. The estuary has a clay mineral sediment assemblage consisting of chlorite, illite and kaolinite, largely derived from suspended fluvial sediment, originating from incision and weathering of the hinterland geology (Daneshvar 2011; Daneshvar and Worden 2016). The southern River Esk drains the Palaeozoic Eskdale Granite; the northern River Irt drains the Triassic Sherwood Sandstone Group and the Borrowdale Volcanic Group;

the central, but minor, River Mite drains a combination of Eskdale Granite, Triassic Sherwood Sandstone Group and the Borrowdale Volcanic Group (Moseley 1978).

MATERIALS AND METHODS

Field-Based Mapping of the Estuary

The estuary was initially mapped by identifying each depositional environment via world imagery and Google Earth. Extensive field mapping and sampling of all geomorphological elements enabled ground-truthing of mapped depositional elements and interpolation using ArcGIS. Tidal flats were further subdivided using the scheme proposed by Dyer (1979), based upon component volume clay fraction (< 2 µm fraction):

0-10 % clay fraction is classed as sand flat,

10-30 % is muddy sand flat,

30-80 % is sandy mud flat.

Surface sediment grain size (approximately 2 cm depth) was determined at 3151 sites in the field using grain size cards and mapped using interpolated in ArcGIS. Lugworm faecal cast density (number per square metre) was recorded in the field using a 1m^2 quadrat, randomly thrown at 3182 sites within the estuary. Lugworm density was mapped across the entire intertidal exposed area, and also mapped using interpolated in ArcGIS. Polished thin sections were constructed from samples across a tidal flat succession to allow mineralogical quantification via automated scanning electron microscope-energy dispersive spectrometry (SEM-EDS). Sediment clay fraction mineralogy was established through X-ray diffraction analysis (XRD).

Determination of Clay Coat Coverage

This study is primarily focused on a suite of 181 surface sediment samples which were subject to grain coat petrography. The sample sites were chosen to provide sufficient spatial coverage and to encompass a fluvial- shallow marine transect incorporating all depositional environments. The clay size fraction volume (weight percentage) was established for 95 of the 181 sites.

Approximately 50 cm^3 of surface sediment was collected at each of the 181 sites. The sediment was then sub-sampled and dried at room temperature. Quantification of detrital clay coverage was achieved using scanning electron microscope (SEM) analysis of grain mounts on a 1 cm diameter stub. The grain mount stubs were examined by SEM petrography in backscattered electron (BSE) imaging.

A complete traverse across each SEM stub was collected by stitching together nine or more BSE images taken for each sample to produce a representative image of approximately 200 grains. In comparison to thin-section based approaches for the study of grain coats, this approach permitted the investigation of detrital-clay coated grains in three dimensions. It also allowed for detailed classification of each sample (Fig. 2). Here we have adopted a novel approach that initially categorises the samples in terms of absence (group 1) or presence (groups 2-5) of clay coat and then subdivides those with coats into the degree of coat coverage (by surface area). Detrital-clay coats within this study were thus categorised into five principle classes:

1) Complete absence of attached clay coats.
2) Less than half of the grains have a small (~ 1-5 %) surface area of attached clay coats.
3) Every grain exhibits at least ~ 5-15 % surface area of attached clay coats.
4) Clay coats observed on every grain with the majority exhibiting extensive (~ 15-30 %) surface area grain coverage.
5) Extensive > 30 % surface area covered by clay coats observed on every grain.

To ensure reliability of the method and interpretation, duplicate SEM stub preparation and analysis was undertaken for 38 of the 181 samples to check the consistency of the classification method. We here note that all replicates faithfully reproduced the initial classification. Critical point drying (Jernigan and McAtee 1975) was not applied to the samples, owing to the absence of delicate fibrous clays associated with authigenic growth.

Clay coat mineralogy

Mineralogical quantification of clay coated sand grains from a mixed sand-mud tidal flat was undertaken via SEM-EDS using an FEI-QEMSCAN® (Armitage et al. 2016). This approach was selected to enable in-situ imaging of clay mineralogy, distribution characteristics and define the link between sediment clay mineralogy and that of clay coats. Three polished thin sections were constructed from surface sediment. The QEMSCAN® system comprises a scanning electron microscope coupled with fast energy dispersive spectrometers (EDS), a microanalyzer and an electronic processing unit, which integrates the data to provide information about the micron scale texture, chemical and mineral composition. The step size for the analysis was 1 µm to ensure that the fine fraction in the sediment was analyzed as well as framework grains.

The data are presented as a combination of a backscatter secondary electron image, and fully quantitative mineralogical content image (framework grains) and quantitative clay mineralogy (total clay, illite, chlorite, kaolinite) to represent the sediment assemblage and component clay-coated sand grains.

Determination of clay fraction

The percentage of the clay fraction (< 2 µm) was established via homogenised sediment sub-samples, dried at 60°C. A few grams of sample were added to 200ml of water and then ultrasonicated for 20 minutes with vigorous stirring at 5 minute intervals. Gravity settling removed sand and silt sized particles, with the supernatant water (containing the clay grain sized particles) decanted and settled by centrifugation to obtain the clay fraction. The separated clay fraction was dried at 60°C, crushed in an agate pestle and mortar and then weighed, revealing the percentage clay fraction within the sediment sample.

Determination of bulk sediment clay fraction mineralogy

Classification of the clay fraction (<2 μm) mineralogy was undertaken by X-ray diffraction analysis (XRD). The clay sized fraction was detached from framework grains using an ultrasonic bath and isolated using centrifuge settling, at 5000 rpm for 10 minutes. The separated clay fraction was dried at 60 degrees and scanned as a randomly orientated powder, using a PANalytical X'Pert Pro MPD X-ray diffractometer. XRD analysis was carried out for the same samples that were mineralogy mapped through (SEM-EDS) analysis.

RESULTS

Surface Sedimentary Characteristics and Distribution of Biological Activity

Sedimentary environments were identified in the field, with further subdivision of the tidal flats based upon the lab-derived clay fraction data sets into sand-flat, muddy sand-flat and sandy mud-flat (Fig. 1).

High resolution, spatial distribution maps of sediment grain size reveal a wide range of mean grain sizes, from very fine to coarse sand sized sediment (Fig. 3A). There is a large scale trend of decreasing grain size away from the ocean, and smaller scale patterns of decreasing grain size with increasing distance from the main ebb channel, towards the tidal limit (Fig. 3A).

A heterogeneous distribution of lugworms occurs in the estuary, as denoted by the widely varying lugworm cast density (Fig. 3C). The lugworm density at the sediment surface is taken to indicate the intensity of bioturbation in the biotic zone of the sediment (McIlroy et al. 2003; Needham et al. 2005). The highest density of lugworms (31 to > 50 per m^2) was observed within the outer sand tidal flats and non-vegetated tidal bar depositional environments (Figs. 1 and 3C). Comparing the sediment grain size map (Fig. 3A) to the lugworm population map (Fig. 3B) suggests that well-developed lugworm populations tend to be confined predominantly to the inner estuary where the sediment grain size tends to be between 88 and 177 µm.

The percentage sediment clay fraction data have been split into eight classes (Fig. 3B). Samples that contain > 1.5 % clay fraction are confined to the inner estuary. Samples that contain < 1.5 % clay fraction sit within the seaward portion of the estuary and outer tidal-flats (Fig. 3B). This pattern suggests that there is an inverse relationship between overall grain size and the amount of co-deposited clay fraction, i.e. there is an increased percentage of the clay fraction with decreasing grain size.

Clay fraction mineralogy

The sediment samples have a clay fraction composed of illite, chlorite and kaolinite, with an average 7.6 % clay fraction in the sediment . X-ray diffraction shows that the clay fraction is dominated by illite (62 % of the clay fraction) clay with chlorite (17 % of the clay fraction) and kaolinite (21 % of the clay fraction) expressing similar values. (Fig.4).

Characteristics of Detrital-clay coats

The observed detrital-clay coated grains are generally characterised by thin and discontinuous accumulations of individual but interlocking (overlapping and aligned clay platelets) clay minerals (Fig. 5). This study has focussed on the morphology of the coat and here we do not rely on a differentiation based on internal structure. Each sample was characterised by the morphology of the coat, the extent (degree) of grain coverage and abundance (proportion of grains that contain coats) (Figs. 2). The clay coats occur on both convex and concave grain faces but the coats with the greatest thickness (maximum of about 5 µm) occur in grain indentations (Fig. 5G, 6E, 7). Clay coats occupy up to about 60 % surface area of individual grains in a given sample.

Detrital-clay coats are composed of individual interlocking clay minerals with a mixed mineralogy even along a singular ridge structure and a range of accessory impurities consisting of silt-sized quartz and bioclastic debri. Clay coats have been observed on all component framework grains within the sediment assemblage (quartz, feldspar, dolomite, calcite). The sand grains within this study are coated with a mixture of clay minerals (Fig. 7), dominated by illite (9.1 image area percentage), with minor chlorite (1.7 image area percentage) and kaolinite (1.1 image area percentage). There was no identified variability between clay mineralogy and component clay coat morphological classes (ridged, bridged, and clumped).

Detrital-clay coats occur with a variety of morphologies (Fig. 5). Here, we have grouped the samples into three principle morphological classes: ridged, bridged and clumped (Fig. 6).

Ridged clay coats consist of elongate intergrowths of plate-like clay minerals, orientated at high angles to the grain surface (Fig. 6A). Ridged coats have variable lengths (< 200 µm) and are preferentially observed upon relatively flat grain surfaces with minimal (silt) impurities. Ridged clay coated grains predominantly occur within the coarser, cleaner sediment assemblages that are associated with outer tidal flat and non-vegetated tidal bar environments.

Bridged clay coat textures occur between detrital grains. Bridged clay coats consist of elongate clay mineral aggregates that connect two grains. Bridged clay coats are relatively uncommon within surface sediment, possibly as result of the sampling procedure (Fig. 6B).

Clumped clay coats are highly variable both in extent and thickness (Fig. 5 and 6C). Clumped coatings are commonly reach sizes of up to 200 µm, and contain silt-sized fragments as well as clay grade material. Clumped clay coats are most abundant within the upper estuary intertidal muddy sand flats, tidal bars and salt marsh depositional environments.

Spatial Distribution of Detrital-Clay Coated Grains

There is a high degree of variability in the distribution of detrital-clay coated grains, although most outer estuary sediment exhibits no more than minor attached clay coats (Fig. 8). The proportion of detrital-clay coated grains in the estuary tends to increase with distance from the open ocean and with distance from the main ebb channel. Clay coats are most extensive within the upper reaches of the three estuary channels. There is a strongly heterogeneous distribution of clay coat classes within the southern Esk estuary arm, while the northern Irt and central Mite estuary arms show more homogeneous distributions. In the central and sea-ward portions of the estuary, clay coats tend to be either absent or present in trace amounts (classes 1 and 2).

The surface sediment samples have here been plotted against depositional environment, with the aim of allowing the modern clay coat data to be compared to ancient, deeply buried sediments (Fig. 9). Detrital-clay coated grains are present within the fluvial channel sediments ranging from absent (class 1) to extensive (class 4) depending upon the position of the sample relative to the channel axis. Grains from inner meander and point bars samples typically have better developed clay coats representative of class 3-4. Grains from fluvial overbank samples tend to have the best developed detrital-clay coats on grains (class 3-5).

Inner estuary tidal depositional environments have a heterogeneous pattern of detrital-clay coated grain coverage. Clay coats are more extensively developed on detrital grains within vegetated, as opposed to non-vegetated, tidal bars (Fig. 9). Tidal flats (sand flat, muddy sand flat, sandy mud flat) represent the only inner estuary depositional environment in which the full spectrum of clay coat grain coverage has been observed (classes 1 to 5). Samples that contain >10% clay fraction correspond to muddy sand flats. All grains in all samples from muddy sand flats contain some degree of clay coating. Samples from sandy mud flat (with >30% clay fraction) contain extensive (class 4-5) detrital-clay coat grain coverage. Saltmarsh sediment assemblages have uniformly well-developed detrital-clay coats (class 5). The observed variability in detrital-clay coat characteristics within tidal environments correlates to grain size; the more extensively developed detrital-clay coats (class 4-5) occur within very fine sand grain size dominated sediment (e.g. compare Fig. 8 to Fig 3A).

The samples from foreshore, ebb delta, tidal inlet and eolian dune depositional environments largely do not contain detrital-clay coated grains. Most samples from the vegetated, dune-topped spits and sheltered region within the tidal inlet contained no clay coat coverage (class 1) and the remainder had minor clay coat coverage (class 2) (Fig. 9).

Detrital-Clay Coated Grains: Grain Size, Clay Fraction and Bioturbation

Bin class intervals have been plotted against average grain size, percentage clay fraction and lugworm density (Fig. 10). This confirms that there is increasing percentage clay fraction with decreasing grain size. This also shows that increasing the percentage of the clay fraction correlates with increasing clay coat coverage (class number). Thus, clay coat class 3 (every grain exhibiting at least ~5-15 % attached clay coats) corresponds to sediment with a 2.5% clay fraction, while clay coat class 5 (extensive, >30 %, clay coats observed on every grain) corresponds to sediment with 10% clay fraction (Fig. 10). The coverage of clay coats does not seem to simply relate to lugworm density with the two highest clay coat classes found in association with low lugworm densities (Fig. 10).

Detrital-clay coats vary systematically within a given depositional environment (Fig. 9). Extensive detrital-clay coated grains are observed within the inner estuary tidal depositional environments, and they increase in extent towards the upper tidal limit (Figs. 8 and 9). Variations in grain size and clay fraction are secondary controls, with a lower fine sand grain size and >5 % clay fraction required to form uniform-extensive detrital-clay coats upon grains (class 3-5). There are negligible attached clay coats (class 1-2) observed within the high energy (upper fine-lower medium grain size), clean (<2% clay fraction) sand assemblages of the outer sand tidal flat, foreshore, ebb delta and eolian dune environments.

DISCUSSION

Origin of Detrital-clay coat Textures

The internal fabric and outer morphology of clay coats in deeply buried reservoir have been described in a few studies. Clay coats tend to be composed of an inner, densely packed, tangentially oriented, root layer that tends to be overlain by an outer coat composed of perpendicular euhedral flakes that grow into open pore spaces (Ajdukiewicz and Larese 2012; Wise et al. 2001). It has been proposed that the inner layers are the result of thermally-driven recrystallization of precursor detrital-clay coats (Aagaard et al. 2000; Billault et al. 2003). The clay coats from the Ravenglass Estuary, described here, are therefore analogues for the inner layer of clay coats reported from deeply buried reservoirs.

The observed ridged and bridged textures within this study (Fig. 6A, B, 7) have been reported previously in a range of case studies (Dowey 2013; Franks and Zwingmann 2010; Houseknecht 1992; Matlack et al. 1989; Moraes and De Ros 1992; Wilson 1992) and in synthesis experiments (Matlack et al. 1989). Ridged detrital-clay coat textures have been interpreted to derive from infiltration processes (Wilson 1992); bridge structures have been reported to form where ridges join two adjacent grains; initially bridged structures develop distinct ridged texture when the sediment is disaggregated (Matlack et al. 1989). The sediment from the Ravenglass Estuary exhibits many of the textural characteristics that have been reported to result from clay infiltration into sand-dominated sediment (Wilson 1992). Infiltrated ridged detrital-clay coat textures have been reported within the Brazos River and Galveston marginal marine system, Texas (Matlack et al. 1989), as well as in the Anllons Estuary, Spain and Leiravogur Estuary, Iceland (Dowey 2013).

Infiltration occurs when water that contains suspended clay and silt flows into partially water-saturated sandy sediment. Within estuarine settings, infiltration is driven by a hydraulic gradient produced by the effect of the tidal range. This gradient drives suspended clay through the sediment at falling tide, towards the low tidal main ebb channel or during times of flooding due to increased rainfall in the hinterland (Santos et al. 2012). Reduction of flow velocity results in the deposition of the suspended clay and silt particles on to the sand grains (Dowey 2013; Worden and Morad 2003).

Clumped clay coat textures, that are comparable to those illustrated in this study (Fig. 6C), have been reported within the sediment of the Mandovi Estuary, India (Mohan Kessarkar et al. 2010), with similar clump sizes and textures. The subtropical Mandovi Estuary clay coats are composed of clay particles, bioclasts and organics that produce a heterogeneous mineralogy that is reported to be fluvially-derived from weathering products in the hinterland (Mohan Kessarkar et al. 2010). Clumped clay accumulations have also been reported within the fluvial-estuarine Rappahannock River, Virginia (Pierce and Nichols 1986). In both the Rappahannock and Mandovi examples, clumped textures were interpreted to originate from the deposition of biogenic (faecal) pellets and flocculated estuarine aggregates (Crone 1975) under stagnant pore water conditions in the estuary.

A comparison of clay coat textures found in the Ravenglass Estuary to other modern analogues, as well as experimental-based results, suggests that clay coats derive from a combination of infiltration, resulting in the ridged-bridge textures, and flocculation with the deposition of biogenic faecal pellets resulting in clumped textures.

Origin of detrital-clay coat mineralogy: internal or external to the estuary?

The illite-dominated, mixed mineralogy of the clay-coated sand grains, determined by spatially-resolved SEM-EDS (Fig. 7), is consistent with the clay fraction mineralogy identified by XRD (Fig. 4). Had the clay coats formed in the hinterland, a much more varied clay-coat mineralogy would be expected than revealed by micro-studies using SEM-EDS and bulk-studies using XRD. Therefore, the observation that the clay coat mineralogy reflects the bulk clay mineralogy of the estuary implies that the clay coats were formed in the estuary itself rather than in the hinterland.

Detrital-Clay Coat Distribution and Origin

It has been reported that the primary depositional environment of a clastic sediment exerts a strong control on subsequent diagenetic processes, via the sediment texture, primary mineralogy, organic content and aqueous chemistry (Ehrenberg 1997; Morad et al. 2010; Worden and Morad 2003). The concept of a depositional control on the occurrence, type and subsequent diagenetic evolution of detrital-clay coats is reasonably well established (Bloch et al. 2002; Dowey et al. 2012; Ehrenberg 1993; Luo et al. 2009; Matlack et al. 1989). The results of this study confirm a depositional environment control but reveal, for the first time, systematic variability of the extent and completeness of clay coat coverage on a marginal marine depositional sub-environments scale.

Comparison of Clay Coats in Ravenglass to Modern Estuary Studies

In the Ravenglass marginal-shallow marine system, the most extensive detrital-clay coated grains are confined to the inner estuary tidal flat, tidal bar, saltmarsh and fluvial point bar depositional environments. In contrast, detrital-clay coated grains are effectively absent within the coarse, clean sand that is associated with outer tidal flats, foreshore, dune topped spits, fluvial channel axis and main ebb channels. The distributions that are illustrated in Figures 8 to 10 have similarities to that of detrital-clay coated grain distribution along the Texas Gulf Coast, Galveston and within the Brazos River (Matlack et al. 1989). The Texas study reported clay coated grains from fluvial point bars, but an absence of detrital-clay coated grains within beach, delta beach, flood tidal delta, and delta plain surface sediments. Studies of the Anllons Estuary, Spain and Leiravogur Estuary, Iceland undertaken by Dowey (2013), support the observed distribution within this study, with detrital-clay coated grains being best developed within the less marine-influenced, middle and upper estuary reaches related to muddy tidal flats.

Comparison of Ravenglass Clay Coats to Ancient, Deeply Buried Clastic Sediment

Reservoir studies, based on cored wells and interpretation of primary depositional environments, tend to be hampered by a lack of high resolution facies interpretation and relatively poor definition of the spatial and stratigraphic distribution of clay coated grains. To date, there is no published subsurface reservoir dataset that compares to the high spatial resolution and the complete certainty of the depositional environment used in this modern analogue study.

Although morphologically dissimilar, occurring as discontinuous clumps and ridges, broad textural and mineralogical similarities are identifiable between the precursor detrital-clay coats of this study and clay coats in diagenetically-altered reservoirs. Mixed mineralogy has been reported in several reservoirs, for example the Lower Cretaceous Mississauga Formation (Gould et al. 2010) and the Jurassic Garn formation (Storvoll et al. 2002), in which the inner (tangential) diagenetic clay coats consist of a mixed illite-chlorite- mineralogy that is broadly similar to the mixed mineralogy of the detrital-clay coats in Ravenglass (Fig. 7).

In the Upper Carboniferous submarine-fan and marine slope facies of the Arkoma Formation, USA it has been reported that muddy clay coated grain facies offer the best reservoir quality prospects compared to the well-sorted, clean sandstones (with little or no dispersed clays). (Houseknecht 1992). In the Arkoma Formation, amalgamated sandstone units contain beds with clay coated grains and no quartz overgrowth and adjacent clean sandstone beds that are devoid of clay coated grains but with pervasively quartz overgrowth, and therefore have negligible remaining porosity (Houseknecht 1992). Although the environment of deposition is different, the Arkoma example illustrates that a small quantity of clay that is co-deposited with sand can lead to improved reservoir quality.

CONTROLS ON THE FORMATION AND DISTRIBUTION OF DETRITAL-CLAY COATS

In this study, we have produced a high resolution, modern analogue data set and established the distribution patterns of detrital-clay coats relative to surface sedimentary and biological facies. Percentage clay fraction, grain size and bioturbation have all been advocated as controls on the origin of clay coated grains in ancient, deeply buried sandstones.

Role of Grain Size

From this study, the observed inverse relationship of increasing detrital-clay coats coverage with decreasing grain size (Fig. 10) is consistent with previous observations by Wilson (1992), that clay coats are more extensively developed within finer grained sandstones in Holocene eolian dune and marine-shelf settings. The Permian-Carboniferous Unayzah sandstones, Saudi Arabia, also have a reported relationship between mean grain size and the average percentage coverage of grains, with fine- to very fine-sandstone exhibiting the greatest degree of clay coat coverage (Shammari et al. 2010).

Role of Percentage Clay Fraction Control

The role that percentage clay fraction (< 2 µm) plays in the formation and distribution of detrital-clay coated grains is not well established within the literature. However, the Anllóns Estuary, Spain, has a clay fraction percentage that increases in marginal areas towards the upper tidal limit (Dowey 2013), consistent with the present study. The Anllóns example identified a trend comparable with Ravenglass of increasing clay coats coverage with increasing co-deposited clay fraction percentage (Dowey 2013). Furthermore, in the Texas Gulf Coast at Galveston and within the Brazos River, virtually no clay-coated grains occur in environments that are characterised by low suspended sediment concentrations (assumed here to be proportional to the percentage clay fraction) (Matlack et al. 1989).

Bioturbation Control

Sediment bioturbation (specifically ingestion and excretion) has been experimentally shown to lead to the creation of clay coats on detrital sand grains (McIlroy et al. 2003; Needham et al. 2006; Needham et al. 2004; Needham et al. 2005). This mechanism works through the production of a mucus membrane on sand grains which then adheres finer clay-silt sized sediment on to the sand grains.

In the present study, the distribution of clay-coated grains does not spatially correlate with the degree of bioturbation observed in the estuary (compare Fig 3, 8 and see Fig. 10). It is also notable that a similar conclusion can be drawn from the Lower Cretaceous Missisauga Formation, Scotian Basin, where the coverage of clay coated grains does not positively correlate with the degree of bioturbation (Gould et al. 2012). The lack of correlation between bioturbation and the degree of clay coated grains in this study may result from the limited environmental grain size niche of the utilized lugworm biogenic proxy. To address this, a focused study on the abundance distribution of estuarine macro- and microorganisms would be required.

IMPLICATIONS FOR HYDROCARBON EXPLORATION

Target Reservoir Quality Prospects

At depths > 3 km (temperatures > 90°C) pervasive authigenic quartz typically starts to become a dominant cement in sandstones (Bloch et al. 2002). Such sandstones risk becoming extensively quartz cemented if grain coats are absent, or poorly developed, upon grain surfaces (Ajdukiewicz and Larese 2012).

Based upon the surface distribution patterns of detrital-clay coats presented here (Figs. 8-10), the best prospects for anomalously high reservoir quality due to the presence of clay coated grains in deeply buried sandstones (> 3km), should be sought within the fine sand sized sediment that also contains approximately 5% clay fraction percentage. Specifically targeting clay-bearing sandstones in the hunt for elevated porosity is against common convention, which would typically target the cleanest, most clay-free sandstones. Our interpreted optimum value of approximately 5 % clay fraction is based upon the likelihood of producing extensive clay coats within sandstones. However we note that highly elevated clay content would of course produce a detrimental effect on permeability and porosity (see next section). Sites with fine sand-sized sediment that also contain approximately 5% clay fraction correspond to inner estuary tidal bar, tidal flat and fluvial point bar facies in the Ravenglass system. In contrast, coarse, clean sand from tidal channels, outer sand flat and foreshore facies would, upon deep burial, potentially experience pervasive quartz cementation due to the lack of inhibiting detrital-clay coated grains if the sediment reached temperatures sufficient for quartz cementation.

Goldilocks Zone of Optimum Detrital-Clay Coat Coverage

The high resolution, marginal-shallow marine model for the distribution of detrital clay-coated grains presented in this study may be used, by analogy, to help in the prediction of clay coated sandstones in the deep subsurface. Too much clay is highly detrimental to sandstone reservoir quality (Armitage et al. 2016; Houseknecht and Pittman 1992; Worden and Morad 2003) since abundant clay minerals fill pores and block pore throats between sand grains. The quantity of clay in a sandstone that is sufficient to coat grains (and thus inhibit quartz cement) but not enough to block pore throats, surprisingly, remains poorly resolved, and is addressed below.

Bloch et al. (2002) noted that a minor amount of clay (as little as 1 to 2% of the rock volume) can coat a relatively large surface area of sandstone grains, but the optimum amount for specific clay minerals has not been precisely defined. Here examples from previous studies were used to help constrain broad percentages of total clay quantities as clay coats that can lead to the development of diagenetic coats which can successfully inhibit quartz cement. Pittman et al. (1992) suggested an optimum range of 5 to 13 % sediment volume of clays occurring as chlorite grain coats for the Tuscaloosa Formation and 4 to 7 % for the Berea Sandstone. Heald and Baker (1977) reported an optimum range of 3.5 to 6.5 % volume of illite clay coats for reservoir quality within the Rose Run sandstone.

Here, we tentatively propose (from the observed association of clay fraction occurring predominantly as clay coatings) lower and upper threshold values of 3.5 and 13.0 % total volume of clay minerals (chlorite, illite and mixed) as the optimum range for the eventual development of clay coats that can form continuous barriers that prevent quartz cementation and so preserve reservoir quality. Using the 3.5 to 13.0 % range of total volume of clays, we have mapped out regions within the Ravenglass Estuary that would lead to the best reservoir quality, were this sedimentary system to be deeply buried (Fig. 11). These optimum regions, termed “Goldilocks zones”, encompass the central tidal flat region, non-vegetated and upper estuary tidal bar depositional environments.

CONCLUSIONS

1. The work presented here, from the Ravenglass Estuary, UK, represents the first high resolution study of the distribution of detrital-clay coated grains within a modern marginal-shallow marine setting.
2. Sedimentary environment is the main control on the absolute quantity of clay minerals and detrital-clay coat sand grain coverage in these sand-dominated sediments.
3. Detrital-clay coats in recent sediments have discontinuous ridged, bridged and clumped textural morphologies. The coats on sand grains are formed of individual interlocking clay minerals with silt-sized lithic and bioclastic accessory components and were probably derived from a combination of infiltration (of clay-bearing water into sand-dominated sediment), flocculation and biogenic processes. Clay coats range from being absent to covering > 30% of sand grain surfaces in a given sample.
4. The observation that the illite-chlorite-kaolinite clay coat mineralogy reflects the bulk clay mineralogy of the estuary implies that the clay coats were formed in situ within the estuary rather than in the hinterland.
5. The distribution of detrital-clay coated grains is primarily a function of sediment grain size and clay fraction percentage. In the Ravenglass case study, a sediment assemblage composed of fine-grained sand containing > 5 % clay fraction percentage is necessary for the development of uniform-well developed clay coats on detrital grains.

6. The best prospects for anomalously high reservoir quality in deeply buried marginal marine sandstones (i.e. with inhibited growth of quartz cement) should most likely be sought within clay-rich inner estuary tidal facies.

FIGURE CAPTIONS

Figure 1. Location maps. A) The Ravenglass Estuary, within the UK. B) Regional map showing the study area and component depositional environments. Tidal flats have been subdivided based upon their component clay fraction (< 2 µm); 0-10 % sand flat, 10-30 % muddy sand flat, 30-80 % sandy mud flat. Classification modified from the scheme initially proposed by Dyer (1979). The black square indicates the sediment sample location from which clay coat (SEM-EDS) and sediment clay fraction (XRD) mineralogical analyses (Fig.4 and Fig. 5) were undertaken.

Figure 2. SEM electron images showing the variable extent of attached clay coats observed within surface sediment samples, which define the basis of the utilized classification scheme. 1) Complete absence of clay coats. 2) ~1 to 5 % attached clays on less than half of the grains. 3) Every grain exhibits ~5 to 15 % clay coats coverage. 4) Clay coats observed on every grain with the majority exhibiting extensive ~15 to 30 % coverage. 5) Extensive, > 30 % clay coats coverage observed upon every grain.

Figure 3. Distribution maps of surface sedimentary features. A) High resolution map of surface sediment grain size (n = 3150). B) Surface distribution of clay fraction percentage (n = 2000) C) High resolution map of lugworm population in surface sediment (n = 3182).

Figure 4. X-ray diffractogram used to quantify the bulk sediment clay fraction mineralogy of surface sediment within the Ravenglass Estuary (for location, see Fig. 1).

Figure 5. Representative SEM electron images of the textural characteristics of surface clay coated sand grains. Arrows indicate regions of clay coat coverage. Note the extent of the ridged clay coat morphologies composed of interlocking and aligned clay particles (A, B, C, and E). The clumped clay coat aggregates composed of clay minerals, lithics and organics are illustrated within (A, D, G, and F). The textural clay coat characteristic of extending pore

ward are observed within (A, C and F) and with greatest accumulation (thickness) observed within grain indentations (E and G).

Figure 6. Clay coat textures showing the main morphological feature classification observed within surface sediment samples. A) Ridged clay coat. B) Bridged clay coat structure. C) Clumped clay coat. Note greatest thickness of attached coating within the grain indentation (enlarged in F). Arrows indicate regions of clay coat coverage.

Figure 7. Scanning electron microscope-energy dispersive spectrometry (SEM-EDS) image, showing clay coat and bulk sediment mineralogy for within muddy sand flat sediment (for location, see Fig. 1). A) Backscattered electron image. B) SEM-EDS image of framework grain mineralogy. C) SEM-EDS image of the component clay fraction mineralogy. D to F) SEM-EDS images of the distribution of illite, chlorite, and kaolinite. Arrows indicate regions of attached clay coating.

Figure 8. Distribution map of surface clay coated sand grains within the Ravenglass Estuary (n = 195). Plotted are the surface distribution of classified areas in light grey signify at least partial clay coat coverage, with dark grey-black regions indicating extensive surface clay coated sand grains.

Figure 9. Frequency histograms for all sediment samples, divided by depositional environment and clay coat bin class: (A) Total number of samples in each clay coat class. (B) Normalised data to reveal relative importance of different environments for optimum clay coat coverage. Clay coat class 1 and 2 have minimal to compete absence of clay coats.

Figure 10. Average grain size, lugworm population and clay fraction percentage plots for each representative clay coat bin class.

Figure 11. Distribution map indicating the literature-constrained Goldilocks zone of the optimum quantity of total clay (i.e. detrital-clay coated sand grains inhibiting quartz cement but not blocking pore throats).

REFERENCES

AAGAARD, P., JAHREN, J.S., HARSTAD, A.O., NILSEN, O., AND RAMM, M., 2000, Formation of grain-coating chlorite in sandstones. Laboratory synthesized vs. natural occurrences: Clay Minerals, v. 35, p. 261-269.

AINSWORTH, R.B., VAKARELOV, B.K., AND NANSON, R.A., 2011, Dynamic spatial and temporal prediction of changes in depositional processes on clastic shorelines: toward improved subsurface uncertainty reduction and management: AAPG bulletin, v. 95, p. 267-297.

AJDUKIEWICZ, J.M., AND LARESE, R.E., 2012, How clay grain coats inhibit quartz cement and preserve porosity in deeply buried sandstones: Observations and experiments: American Association of Petroleum Geologists Bulletin, v. 96, p. 2091-2119.

AJDUKIEWICZ, J.M., NICHOLSON, P.H., AND ESCH, W.L., 2010, Prediction of deep reservoir quality using early diagenetic process models in the Jurassic Norphlet Formation, Gulf of Mexico: American Association of Petroleum Geologists Bulletin, v. 94, p. 1189-1227.

AL-RAMADAN, K.A., HUSSAIN, M., IMAM, B., AND SANER, S., 2004, Lithologic characteristics and diagenesis of the Devonian Jauf sandstone at Ghawar Field, eastern Saudi Arabia: Marine and Petroleum Geology, v. 21, p. 1221-1234.

ARMITAGE, P.J., WORDEN, R.H., FAULKNER, D.R., BUTCHER, A.R., AND ESPIE, A.A., 2016, Permeability of the Mercia Mudstone: suitability as caprock to carbon capture and storage sites: Geofluids, v. 16, p. 26-42.

BILLAULT, V., BEAUFORT, D., BARONNET, A., AND LACHARPAGNE, J.C., 2003, A nanopetrographic and textural study of grain-coating chlorites in sandstone reservoirs: Clay Minerals, v. 38, p. 315-328.

BLOCH, S., LANDER, R.H., AND BONNELL, L., 2002, Anomalously high porosity and permeability in deeply buried sandstone reservoirs: Origin and predictability: American Association of Petroleum Geologists Bulletin, v. 86, p. 301-328.

BOUSHER, A., 1999, Ravenglass Estuary: Basic characteristics and evaluation of restoration options, Restrad-Td.

COCKER, J., KNOX, W., LOTT, G., AND MILODOWSKI, A., 2003, Petrologic controls on reservoir quality in the Devonian Jauf Formation sandstones of Saudi Arabia: Geofrontier, v. 1, p. 6-11.

CRONE, A.J., 1975, Laboratory and field studies of mechanically infiltrated matrix clay in arid fluvial sediments, University of Colorado.

DANESHVAR, E., 2011, Role of provenance on clay minerals and their distribution in modern estuaries: University of Liverpool, 236 p.

DANESHVAR, E., AND WORDEN, R.H., 2016, Feldspar alteration and Fe minerals: origin, distribution and implications for sandstone reservoir quality in estuarine sediments. In: Armitage, P. J., Butcher, A. R., Churchill, J. M., Csoma, A. E., Hollis, C., Lander, R. H., Omma, J. E. & Worden, R. H. (eds) 2016. Reservoir Quality of Clastic and Carbonate Rocks: Analysis, Modelling and Prediction. : Geological Society, London, Special Publications, v. 435.

DOWEY, P.J., 2013, Prediction of clay minerals and grain coatings in sandstone reservoirs utilising ancient examples and modern analogue studies: University of Liverpool.

DOWEY, P.J., HODGSON, D.M., AND WORDEN, R.H., 2012, Pre-requisites, processes, and prediction of chlorite grain coatings in petroleum reservoirs: A review of subsurface examples: Marine and Petroleum Geology, v. 32, p. 63-75.

Dyer, K.R., 1979, Estuarine hydrography and sedimentation: a handbook, Cambridge University Press Cambridge.
Ehrenberg, S.N., 1993, Preservation of anomalously high-porosity in deeply buried sandstones by grain coating chlorite - examples from the Norwegian continental shelf: American Association of Petroleum Geologists Bulletin, v. 77, p. 1260-1286.
Ehrenberg, S.N., 1997, Influence of depositional sand quality and diagenesis on porosity and permeability: Examples from Brent Group Reservoirs, northern North Sea (vol 67, pg 202, 1997): Journal of Sedimentary Research, v. 67, p. 618-618.
Franks, S.G., and Zwingmann, H., 2010, Origin and timing of late diagenetic illite in the Permian-Carboniferous Unayzah sandstone reservoirs of Saudi Arabia: American Association of Petroleum Geologists Bulletin, v. 94, p. 1133-1159.
Gaupp, R., and Okkerman, J.A., 2011, Diagenesis and reservoir quality of Rotliegend Sandstones in the Northern Netherlands - A review, *in* Grotsch, J., and Gaupp, R., eds., Permian Rotliegend of the Netherlands: Society for Sedimentary Geology Special Publication, p. 193-226.
Gould, K., Pe-Piper, G., and Piper, D.J.W., 2010, Relationship of diagenetic chlorite rims to depositional facies in Lower Cretaceous reservoir sandstones of the Scotian Basin: Sedimentology, v. 57, p. 587-610.
Gould, K.M., Piper, D.J.W., and Pe-Piper, G., 2012, Lateral variation in sandstone lithofacies from conventional core, Scotian Basin: implications for reservoir quality and connectivity: Canadian Journal of Earth Sciences, v. 49, p. 1478-1503.
Grigsby, J.D., 2001, Origin and growth mechanism of authigenic chlorite in sandstones of the lower Vicksburg Formation, south Texas: Journal of Sedimentary Research, v. 71, p. 27-36.
Heald, M.T., and Baker, G.F., 1977, Diagenesis of Mt Simon and Rose Run Sandstones in western West Virginia and southern Ohio: Journal of Sedimentary Petrology, v. 47, p. 66-77.
Houseknecht, D.W., 1992, Clay minerals in Atokan deep-water sandstone facies, Arkoma basin: origins and influence on diagenesis and reservoir quality.
Houseknecht, D.W., and Pittman, E.D., 1992, Origin, diagenesis and petrophysics of clay minerals in sandstones SEPM Special Publication: Tulsa Oklahoma, Society of Economic Paleontologists and Mineralogists.
Jernigan, D.L., and McAtee, J.L., 1975, Critical point drying of electron microscope samples of clay minerals: Clays and Clay Minerals, v. 23, p. 161-162.
Lander, R.H., Larese, R.E., and Bonnell, L.M., 2008, Toward more accurate quartz cement models: The importance of euhedral versus noneuhedral growth rates: American Association of Petroleum Geologists Bulletin, v. 92, p. 1537-1563.
Lloyd, J.M., Zong, Y., Fish, P., and Innes, J.B., 2013, Holocene and Lateglacial relative sea-level change in north-west England: implications for glacial isostatic adjustment models: Journal of Quaternary Science, v. 28, p. 59-70.
Luo, J.L., Morad, S., Salem, A., Ketzer, J.M., Lei, X.L., Guo, D.Y., and Hlal, O., 2009, Impact of diagenesis on reservoir quality evolution in fluvial and lacustrine-deltaic sandstones: evidence from Jurassic and Triassic sandstones from the Ordos Basin, China: Journal of Petroleum Geology, v. 32, p. 79-102.
Matlack, K.S., Houseknecht, D.W., and Applin, K.R., 1989, Emplacement of clay into sand by infiltration: Journal of Sedimentary Petrology, v. 59, p. 77-87.
McIlroy, D., Worden, R.H., and Needham, S.J., 2003, Faeces, clay minerals and reservoir potential: Journal of the Geological Society, v. 160, p. 489-493.
Mohan Kessarkar, P., Purnachandra Rao, V., Shynu, R., Mehra, P., and Viegas, B.E., 2010, The nature and distribution of particulate matter in the Mandovi estuary, central west coast of India: Estuaries and coasts, v. 33, p. 30-44.
Morad, S., Al-Ramadan, K., Ketzer, J.M., and De Ros, L.F., 2010, The impact of diagenesis on the heterogeneity of sandstone reservoirs: A review of the role of depositional facies and

sequence stratigraphy: American Association of Petroleum Geologists Bulletin, v. 94, p. 1267-1309.

Moraes, M.A.S., and De Ros, L.F., 1992, Depositional, infiltrated and authigenic clays in fluvial sandstones of the Jurassic Sergie Formation, Reconcavo Basin, northeastrn Brazil: In: Origin, diagenesis and petrophysics of clay minerals in sandstones (eds. Houseknecht, D.W. and Pittman, E.D.) SEPM Special Publication, v. 47, p. 197-208.

Moseley, F., 1978, The Geology of the Lake District, Occoasional Publication: Leeds, Yorkshire Geological Society, p. 284.

Needham, S.J., Worden, R.H., and Cuadros, J., 2006, Sediment ingestion by worms and the production of bio-clays: a study of macrobiologically enhanced weathering and early diagenetic processes: Sedimentology, v. 53, p. 567-579.

Needham, S.J., Worden, R.H., and McIlroy, D., 2004, Animal-sediment interactions: the effect of ingestion and excretion by worms on mineralogy: Biogeosciences, v. 1, p. 113-121.

Needham, S.J., Worden, R.H., and McIlroy, D., 2005, Experimental production of clay rims by macrobiotic sediment ingestion and excretion processes: Journal of Sedimentary Research, v. 75, p. 1028-1037.

Ozkan, A., Cumella, S.P., Milliken, K.L., and Laubach, S.E., 2011, Prediction of lithofacies and reservoir quality using well logs, Late Cretaceous Williams Fork Formation, Mamm Creek field, Piceance Basin, Colorado: American Association of Petroleum Geologists Bulletin, v. 95, p. 1699-1723.

Pierce, J., and Nichols, M.M., 1986, Change of particle composition from fluvial into an estuarine environment: Rappahannock River, Virginia: Journal of coastal research, p. 419-425.

Pittman, E.D., Larese, R.E., and Heald, M.T., 1992, Clay coats: occurrence and relevance to preservation of porosity in sandstones: In: Origin, diagenesis and petrophysics of clay minerals in sandstones (eds. Houseknecht, D.W. and Pittman, E.D.) SEPM Special Publication, v. 47, p. 241-255.

Santos, I.R., Eyre, B.D., and Huettel, M., 2012, The driving forces of porewater and groundwater flow in permeable coastal sediments: A review: Estuarine, Coastal and Shelf Science, v. 98, p. 1-15.

Shammari, S., Franks, S., and Soliman, O., 2010, Depositional and Facies Controls on Infiltrated/Inherited Clay Coatings: Unayzah Sandstones, Saudi Arabia: GEO 2010.

Storvoll, V., Bjorlykke, K., Karlsen, D., and Saigal, G., 2002, Porosity preservation in reservoir sandstones due to grain-coating illite: a study of the Jurassic Garn Formation from the Kristin and Lavrans fields, offshore Mid-Norway: Marine and Petroleum Geology, v. 19, p. 767-781.

Wilson, M.D., 1992, Inherited grain-rimming clays in sandstones from eolian and shelf environments: their origin and control on reservoir properties: In: Origin, diagenesis and petrophysics of clay minerals in sandstones (eds. Houseknecht, D.W. and Pittman, E.D.) SEPM Special Publication, v. 47, p. 209-225.

Wise, S., Smellie, J., Aghib, F., Jarrard, R., and Krissek, L., 2001, Authigenic smectite clay coats in CRP-3 drillcore, Victoria Land Basin, Antarctica, as a possible indicator of fluid flow: a progress report: Terra Antartica, v. 8, p. 281-298.

Worden, R.H., and Morad, S., 2000, Quartz cementation in sandstones: a review of the key controversies In: Quartz cementation in sandstones (eds. Worden, R.H. and Morad, S.) International Association of Sedimentologists Special Publications, p. 1-20.

Worden, R.H., and Morad, S., 2003, Clay minerals in sandstones: Controls on formation, distribution and evolution: In: Clay mineral cements in sandstones (eds. Worden, R.H. and Morad, S.) International Association of Sedimentologists Special Publications, v. 34, p. 3-41.

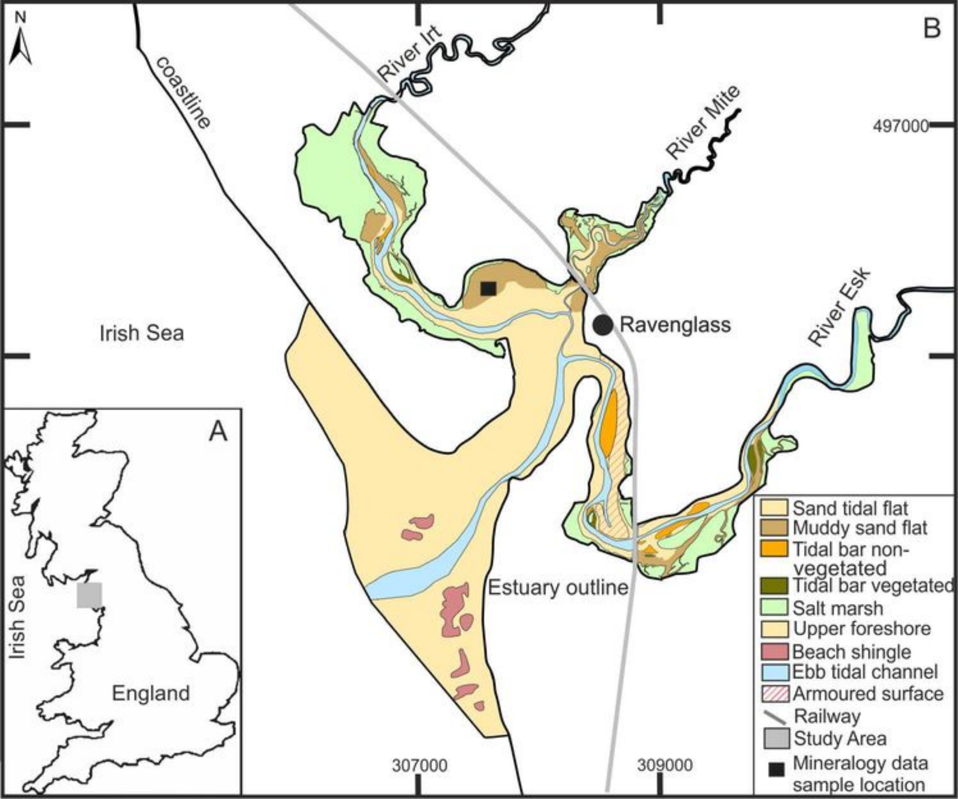
N
B
coastline
River Irt
River Mite
River Esk
497000
Irish Sea
Ravenglass
Estuary outline
307000
309000
A
Irish Sea
England
Sand tidal flat
Muddy sand flat
Tidal bar non-vegetated
Tidal bar vegetated
Salt marsh
Upper foreshore
Beach shingle
Ebb tidal channel
Armoured surface
Railway
Study Area
Mineralogy data sample location

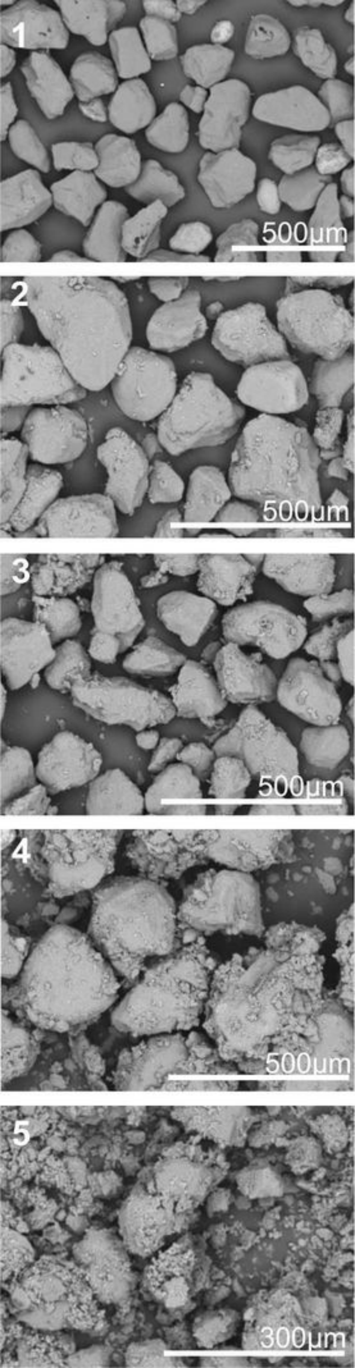
1
500µm
2
500µm
3
500µm
4
500µm
5
300µm

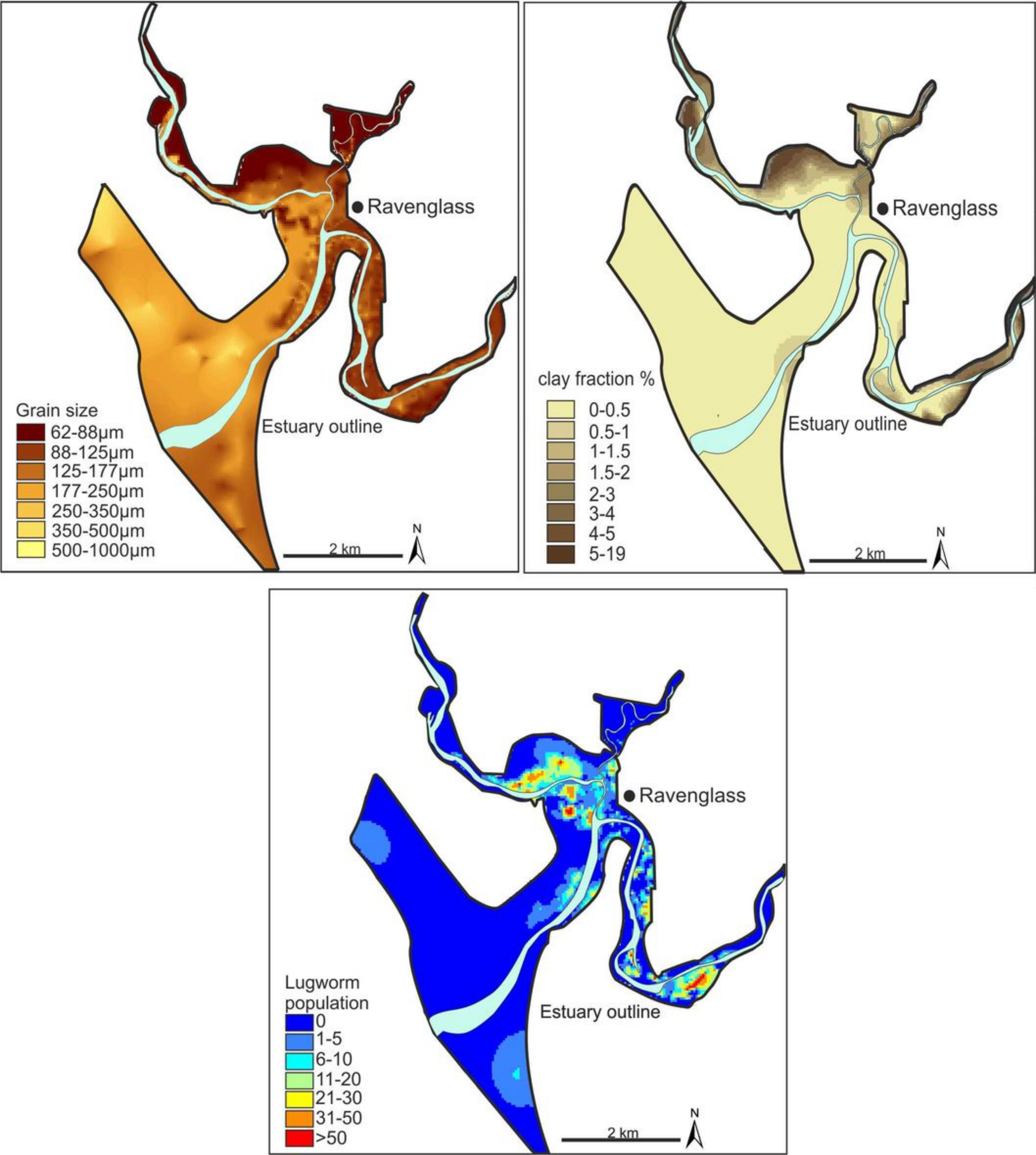
Ravenglass
Estuary outline
Grain size
62-88μm
88-125μm
125-177μm
177-250μm
250-350μm
350-500μm
500-1000μm
2 km
N
Ravenglass
clay fraction %
0-0.5
0.5-1
1-1.5
1.5-2
2-3
3-4
4-5
5-19
Estuary outline
2 km
N
Ravenglass
Lugworm population
0
1-5
6-10
11-20
21-30
31-50
>50
Estuary outline
2 km
N

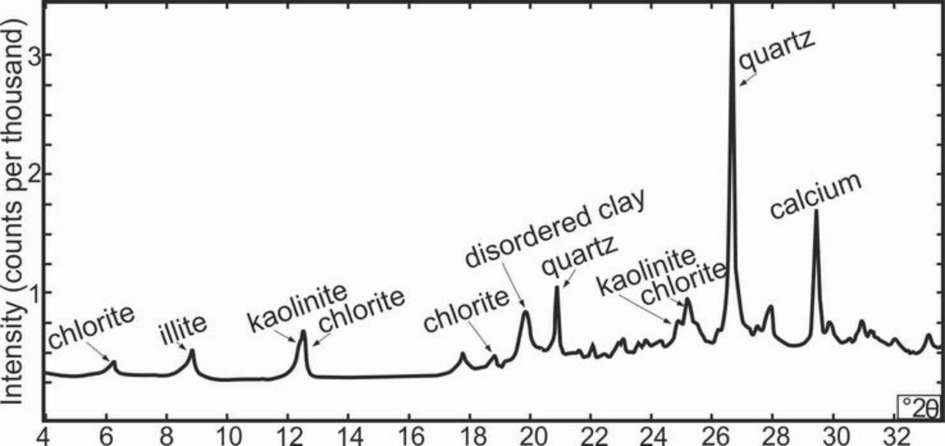
Intensity (counts per thousand)
3
2
1
chlorite
illite
kaolinite
chlorite
chlorite
disordered clay
quartz
kaolinite
chlorite
quartz
calcium
°2θ
4
6
8
10
12
14
16
18
20
22
24
26
28
30
32

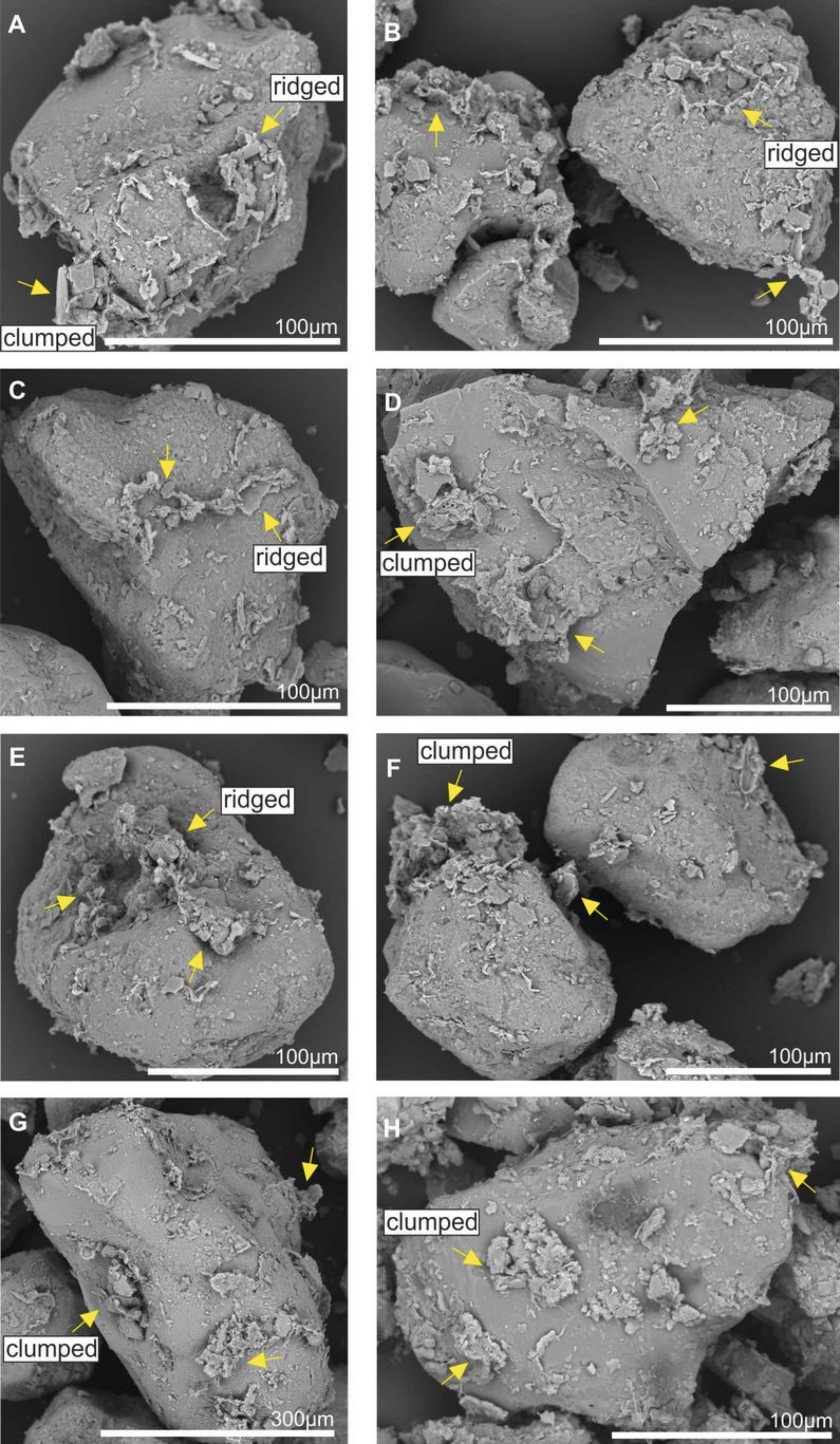
A
ridged
clumped
100µm
B
ridged
100µm
C
ridged
100µm
D
clumped
100µm
E
ridged
100µm
F
clumped
100µm
G
clumped
300µm
H
clumped
100µm

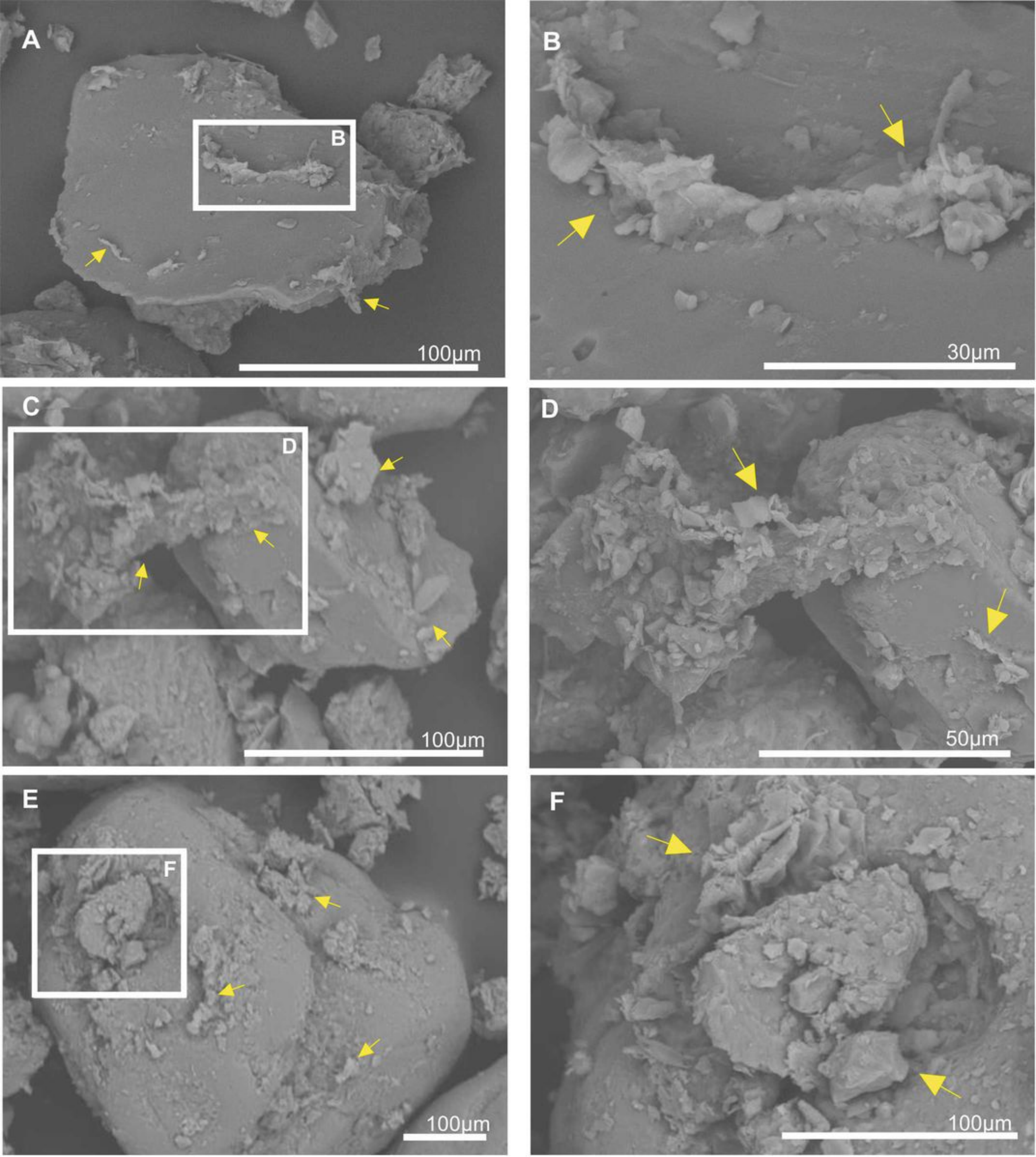
A
B
100μm
B
30μm
C
D
100μm
D
50μm
E
F
100μm
F
100μm

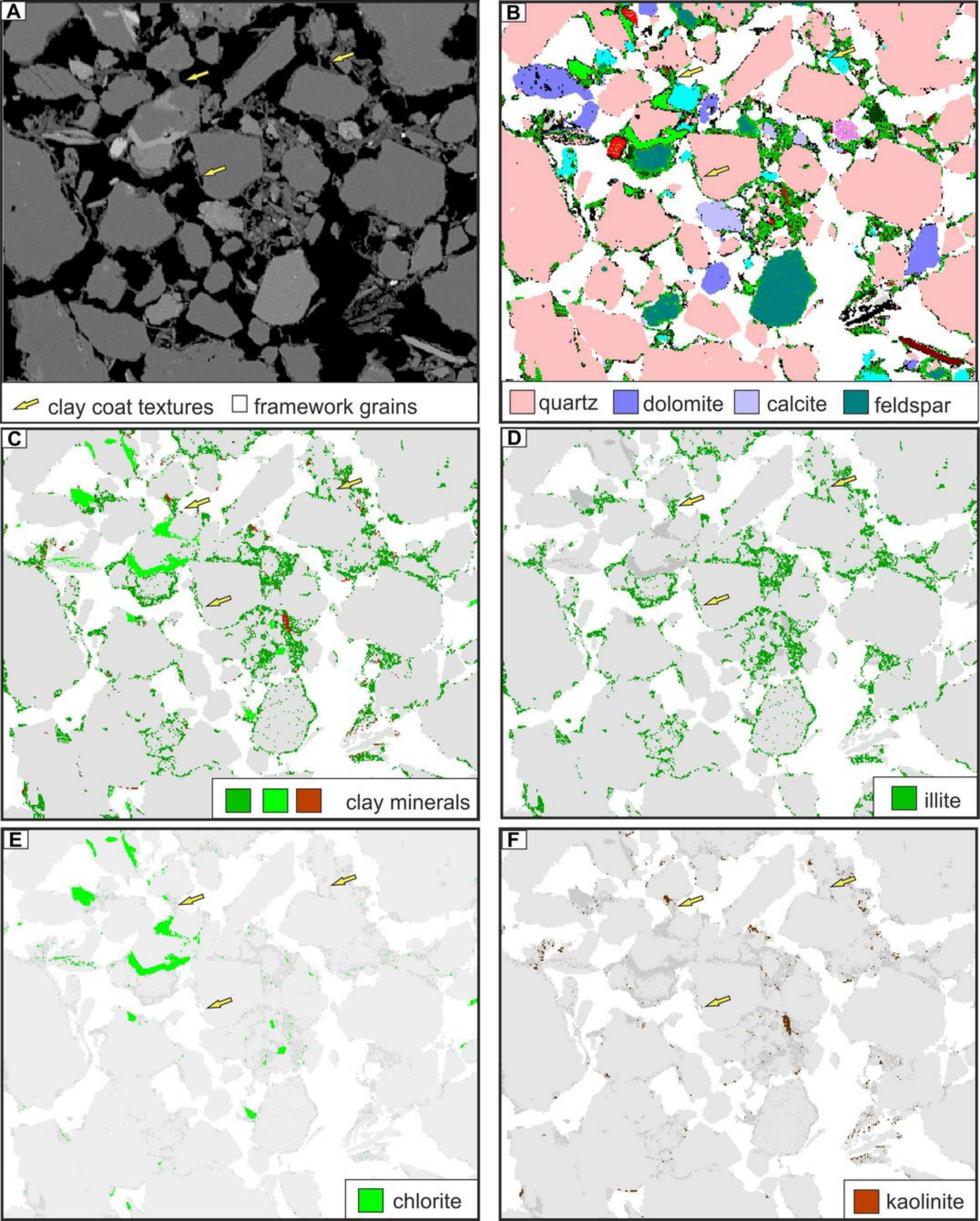
A
clay coat textures
framework grains
B
quartz
dolomite
calcite
feldspar
C
clay minerals
D
illite
E
chlorite
F
kaolinite

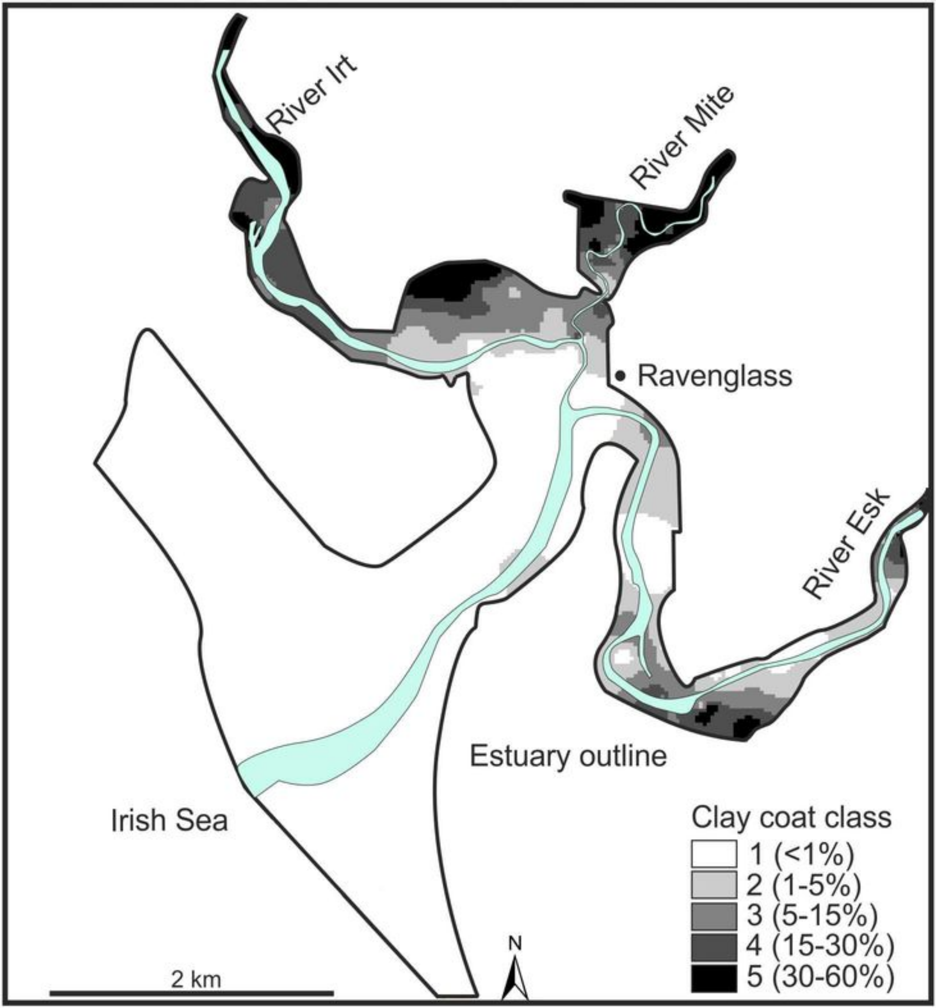
River Irt
River Mite
Ravenglass
River Esk
Estuary outline
Irish Sea
Clay coat class
1 (<1%)
2 (1-5%)
3 (5-15%)
4 (15-30%)
5 (30-60%)
N
2 km

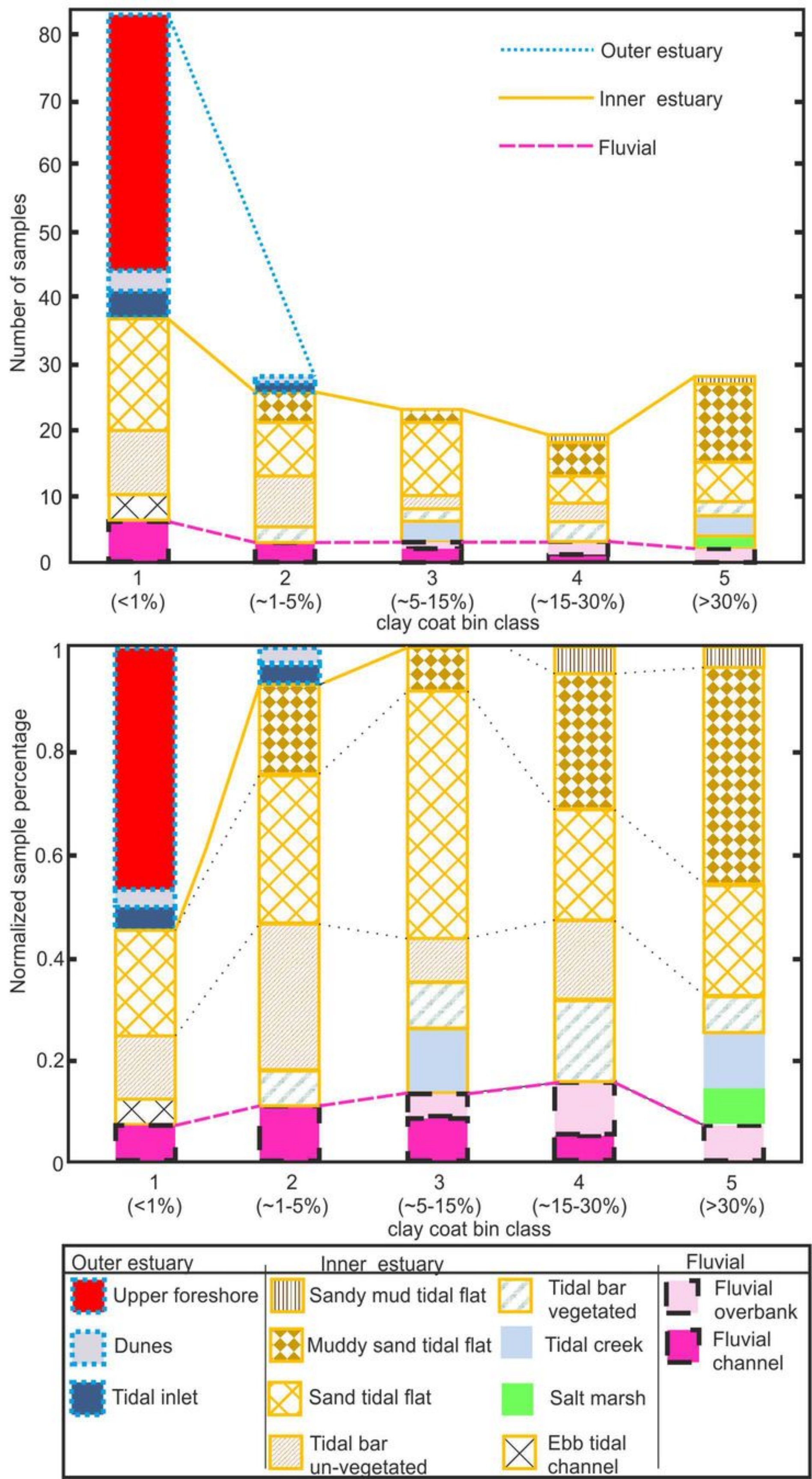

Outer estuary
Inner estuary
Fluvial
Number of samples
clay coat bin class
1 (<1%)
2 (~1-5%)
3 (~5-15%)
4 (~15-30%)
5 (>30%)
Normalized sample percentage
Outer estuary
Upper foreshore
Dunes
Tidal inlet
Inner estuary
Sandy mud tidal flat
Muddy sand tidal flat
Sand tidal flat
Tidal bar un-vegetated
Tidal bar vegetated
Tidal creek
Salt marsh
Ebb tidal channel
Fluvial
Fluvial overbank
Fluvial channel

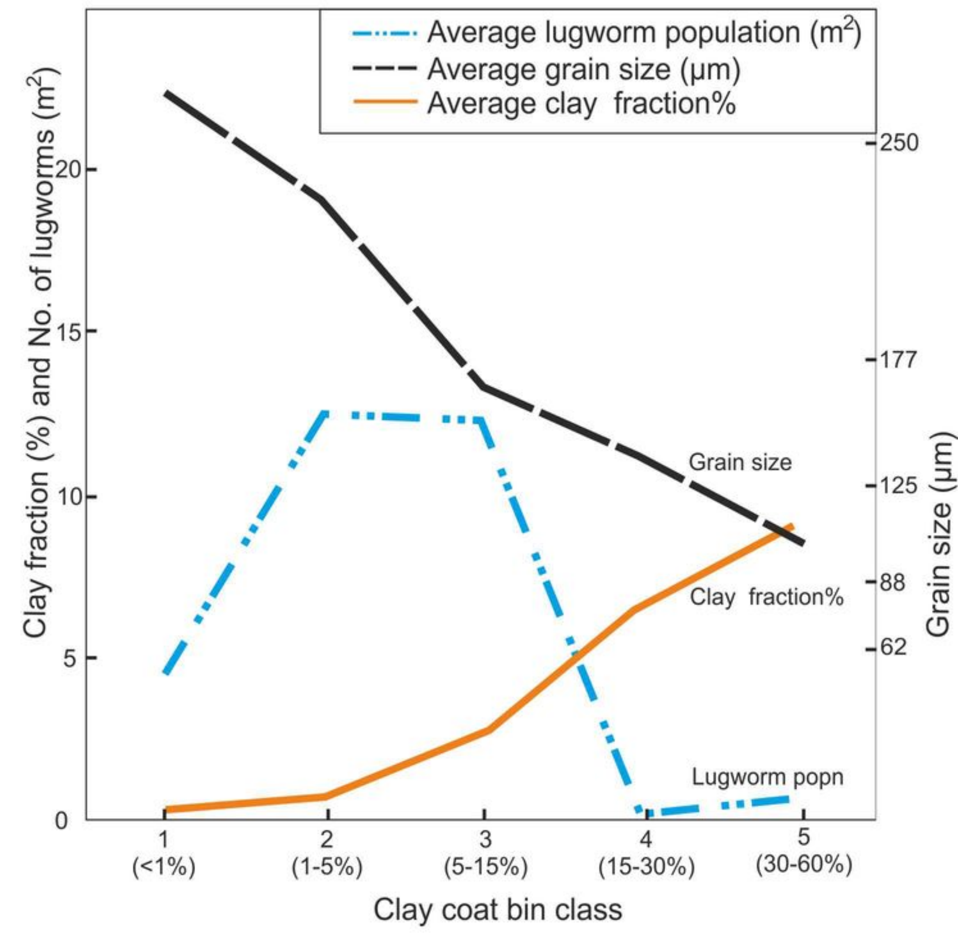

Average lugworm population (m2)
Average grain size (µm)
Average clay fraction%
Clay fraction (%) and No. of lugworms (m2)
20
15
10
5
0
250
177
125
88
62
Grain size (µm)
Grain size
Clay fraction%
Lugworm popn
1
(<1%)
2
(1-5%)
3
(5-15%)
4
(15-30%)
5
(30-60%)
Clay coat bin class

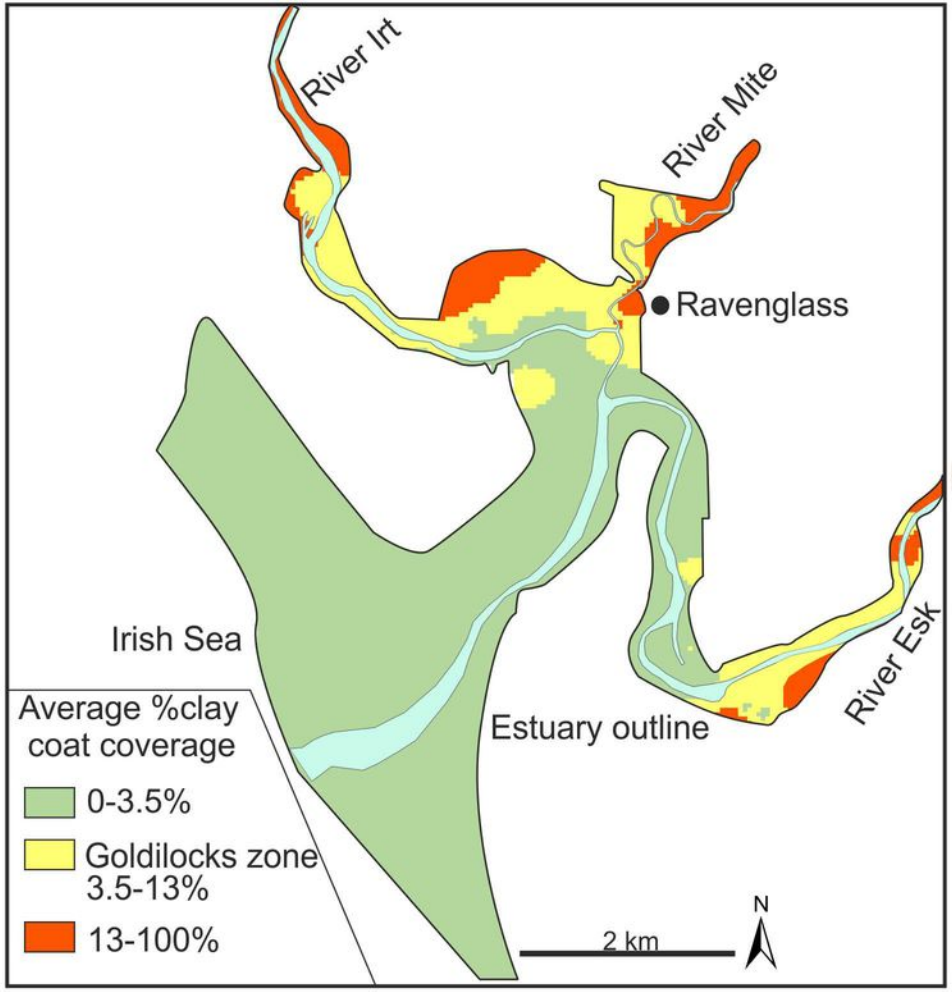
River Irt
River Mite
Ravenglass
Irish Sea
Estuary outline
River Esk
Average %clay coat coverage
0-3.5%
Goldilocks zone 3.5-13%
13-100%
2 km
N